A Control Strategy for Islanded Microgrids With DC-Link Voltage Control

Tine L. Vandoorn, *Student Member, IEEE*, Bart Meersman, *Student Member, IEEE*, Lieven Degroote, *Student Member, IEEE*, Bert Renders, *Member, IEEE*, and Lieven Vandevelde, *Senior Member, IEEE*

***Abstract*—New opportunities for optimally integrating the increasing number of distributed-generation (DG) units in the power system rise with the introduction of the microgrid. Most DG units are connected to the microgrid via a power-electronic inverter with dc link. Therefore, new control methods for these inverters need to be developed in order to exploit the DG units as effectively as possible in case of an islanded microgrid. In the literature, most control strategies are based on the conventional transmission grid control or depend on a communication infrastructure. In this paper, on the other hand, an alternative control strategy is proposed based on the specific characteristics of islanded low-voltage microgrids. The microgrid power is balanced by using a control strategy that modifies the set value of the rms microgrid voltage at the inverter ac side as a function of the dc-link voltage. In case a certain voltage, which is determined by a constant-power band, is surpassed, this control strategy is combined with P/V-droop control. This droop controller changes the output power of the DG unit and its possible storage devices as a function of the grid voltage. In this way, voltage-limit violation is avoided. The constant-power band depends on the characteristics of the generator to avoid frequent changes of the power of certain DG units. In this paper, it is concluded that the new control method shows good results in power sharing, transient issues, and stability. This is achieved without interunit communication, which is beneficial concerning reliability issues, and an optimized integration of the renewable energy sources in the microgrid is obtained.**

***Index Terms*—DC-link voltage control, distributed generation, microgrid, power sharing, P/V-droop, voltage-source inverter.**

I. Introduction

DUE TO limitations of centralized power planning and risks of the volatile bulk power market, small-scale generation next to the centralized generation is gaining interest [1]. Also, the investments in distributed-generation (DG) units are largely stimulated by the technological developments, the increased public interest in distributed renewables, and the reduced cost. Therefore, the number of DG units emerging in the distribution system is largely increasing and with such high penetration of DG units, the fit-and-forget principle of integrating them into the grid is no longer a sustainable option and a coordinated approach is required.

New opportunities for the coordinated operation of DG units rise with the introduction of the microgrid. A microgrid is an interconnection of supply, loads and storage, providing power and heat [2], [3]. A significant share of the electrical devices uses a power-electronic interface for the coupling with the microgrid. An important advantage is that the microgrid elements are collectively regarded by the distribution network as a controlled entity within the power system. Furthermore, microgrids can facilitate the penetration of renewables and other forms of DG into the utility grid and help in power-quality (PQ) issues [3]–[5]. Two operating conditions are possible: grid-connected mode and islanded mode. In the grid-connected mode, the microgrid supports the utility grid while exchanging power with it. In the islanded operation, the microgrid elements are responsible for maintaining the integrity of the microgrid without the assistance of a main grid, which is the focus of this paper. An islanded microgrid can be due to either planned maintenance operations or switching incidents, such as an outage of the main grid or PQ problems [6]. An islanded microgrid can also exist in case of remote electrification, where no main grid is available due to, for example, geographical issues.

Islanded microgrids have very different characteristics in comparison with the conventional electrical systems and, therefore, different operation and control are required [7], [8]. As the microgrid elements are mainly power-electronically interfaced, the microgrid control depends on the inverter control. Inverter control can be divided into two types: PQ control and power-sharing control. In PQ control, the DG unit injects all the available power into the microgrid, usually with unity power factor. A power-sharing control, such as droop control, can be implemented for dispatching the output power [5], [9], [10].

The power-sharing strategy of the DG units in the islanded microgrid can vary from fully centralized to fully decentralized. In [10]–[12], a control principle for islanded microgrids with a microgrid central controller (MGCC), microgenerator controllers (MC), and load controllers (LC) are presented. In a centralized operation, the LC and MC receive set points from the MGCC and a critical communication system is required. In case of a decentralized system, the control decisions are made by the LC and MC locally [8], [11]. A multi-agent system can be applied to control the microgrid with a minimum of data exchange and computational burden. For example, in [7], some control strategies using nested control loops and mostly with master and slave inverters are described. These controllers use

Manuscript received August 07, 2009; revised July 07, 2010 and October 15, 2010; accepted November 17, 2010. Date of publication January 10, 2011; date of current version March 25, 2011. This work was supported by the Belgian Government. The work of T. L. Vandoorn was supported under a Ph.D. fellowship by FWO-Vlaanderen (Research Foundation-Flanders, Belgium). Paper no. TPWRD-00594-2009.

The authors are with the Department of Electrical Energy, Electrical Energy Laboratory (EELAB), Systems and Automation (EESA), Ghent University, Ghent B-9000, Belgium (e-mail: Tine.Vandoorn@UGent.be).

Digital Object Identifier 10.1109/TPWRD.2010.2095044

low-bandwidth communication, that is often not absolutely necessary, but enables better sharing of duty in transient conditions.

A conventional way of decentralized microgrid control where an expensive communication system is avoided, is the active power/frequency (P/f)-droop control, based on the conventional grid control in the transmission system [3], [8], [9], [13]–[17]. In case of multiple inverters, the power will be shared between the generators based on their droop characteristics. However, in contrast with measurements of power, accurate measurements of frequency are not straightforward. Therefore, a control method analogous to the P/f-droop control can be applied with frequency as a function of the delivered active power [13], as opposed to the conventional control that changes the active power as a function of the frequency. However, inverter-interfaced microgrids lack the significant inertia upon which the active power control in the conventional system is based. Therefore, P/V-droops are presented in [13]. These droops are based on the principle that the active power through a microgrid line mainly depends on the voltage amplitude, because low-voltage distribution networks are mainly resistive. In [18] and [19], this P/V-droop control is further developed for multiple voltage-source inverters (VSIs) in parallel.

Most control principles are based on the conventional transmission system control or depend on (minimal) communication. In contrast, the control strategy of islanded microgrids presented in this paper operates without interunit communication in a fully distributed manner and takes the specific characteristics of the microgrid into account. These characteristics include the lack of rotating inertia, resistive line characteristics, and high share of renewables, which are less controllable than the central generators and which require an optimal power exploitation. The active power is balanced by means of a $V_{\rm g}/V_{\rm dc}$-droop control, with $V_{\rm g}$ the rms microgrid voltage and $V_{\rm dc}$ the dc-link voltage, that changes $V_{\rm g}$ according to changes of $V_{\rm dc}$. This modifies the power flow of the DG unit to the microgrid while keeping its generated power constant. Further, in case the voltage exceeds a certain level, the constant-power band, also a $P/V_{\rm g}$-droop control algorithm, is turned on that changes the output power P of the source in order to avoid voltage limit violation. This constant-power band depends on the nature of the power source to fully exploit the power flexibility of the controllable units while optimizing the output of renewable power sources and still enabling changes of their output power. It will be shown that with the combination of the $V_{\rm g}/V_{\rm dc}$ and $P/V_{\rm g}$-droop control strategies, a fully distributed microgrid operation and good power balancing and power sharing are achieved. Also, it enables using the renewable energy more optimally.

In Section II, the microgrid architecture is introduced. In Section III, the $V_{\rm g}/V_{\rm dc}$ droop control strategy and its combination with $P/V_{\rm g}$ droop control are presented as well as their advantages. Also, the principle and advantages of using a constant-power band are presented. In Sections IV and V, some simulation results with these control principles are shown.

II. Microgrid Configuration

In this paper, the microgrid architecture of Fig. 1 is considered. The microgrid is shown from the perspective of a generator; thus, the rest of the system is represented as a black box. The sources of the microgrid have a voltage-source inverter (VSI) interface for the transport of power from the dc side to the ac side. An LC filter is present at the ac side of the VSI in order to attenuate switching ripple. The dc side of the VSI consists of a dc-link capacitor $C_{\rm dc}$ and a power-controlled source $P_{\rm dc}$ or a current-controlled source $I_{\rm dc}$. The microgrid can consist of one or multiple power sources. A single-phase system is considered, but the control strategies can easily be extended for three-phase microgrids. However, then, PQ issues, such as voltage unbalance, should also be taken into account, which is not the focus of this paper. In the simulations, Matlab Simulink is used, combined with the Plecs library to include the VSI switches.

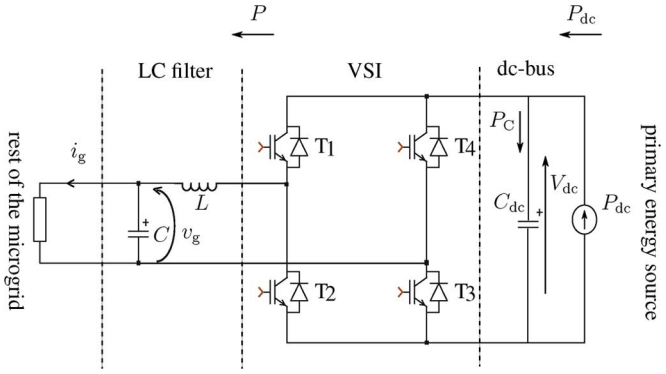

Fig. 1. Microgrid architecture for the case of one power source: ac side (LC filter and rest of the microgrid) as well as VSI and dc side (DG).

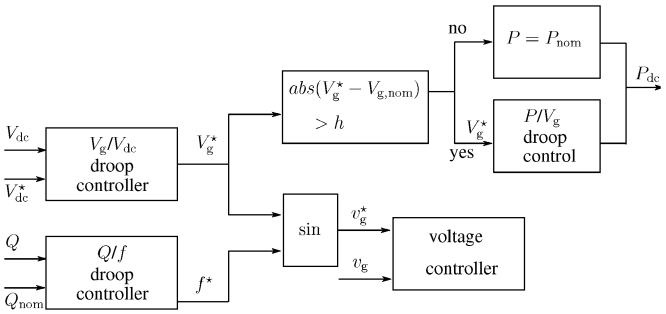

Fig. 2. Microgrid voltage control: $V_{\rm g}/V_{\rm dc}$-droop control and LQR ('$\star$' denotes set values $v_{\rm g}$ microgrid voltage, and h determines the constant-power band).

The microgrid control principle is depicted in Fig. 2, including the outer $V_{\rm g}/V_{\rm dc}$-droop control loop that forms the set value for the inner voltage-control loop. Based on the measurements of $v_{\rm g}$ and the inverter current, the desired microgrid voltage is tracked by using the linear-quadratic regulator (LQR) method [20]. In an LQR, a cost function is minimized, which depends on the tracking error and the tracking labor. By solving the Riccati equation, the state feedback is determined for the control. Here, LQR is proposed since it shows good tracking performance and provides good results concerning stability issues. Other controllers, such as proportional-integral controllers or controllers based on fuzzy logic, can also be implemented [21].

Fig. 2 also shows the inputs and outputs of the controllers and the combination of $V_{\rm g}/V_{\rm dc}$ and $P/V_{\rm g}$ droop control, which will be elaborated on in Section III. For the reactive power control of the generators, a Q/f droop controller according to [22] and

[23] is used. This paper deals with the islanded operating condition. For control in grid-connected and islanded operation, including the transition of modes, two main options are possible. First, a change of control principle can be included. For this, island detection is a main issue and different detection methods are developed [24], [25]. Second, the controllers can be adjusted to operate in grid-connected and islanded operation [26]–[29].

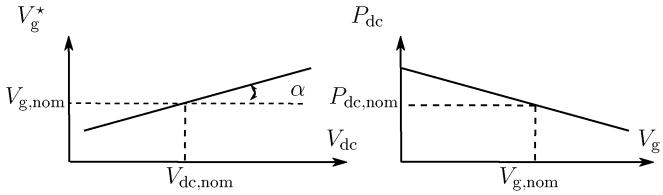

Fig. 3. V_g/V_{dc}-droop and P/V_g-droop.

III. Control Strategy for the Active Power

In this paragraph, the novel control strategy, based on a combination of the V_g/V_{dc}-droop and P/V_g-droop control strategies is presented for the active power management in islanded microgrids.

A. V_g/V_{dc}-Droop Control

The V_g/V_{dc}-droop control principle is based on the specific characteristics of islanded microgrids that differ significantly from those of the conventional power system.

First, islanded microgrids lack the significant inertia of the conventional power system because the microgrid elements are mainly power electronically interfaced. In conventional grids, in short time, the power is balanced by this rotating inertia in the system, resulting in a change of frequency, upon which the conventional power control is based. In the microgrid on the other hand, if an unbalance occurs between the generated power and the absorbed power, the dc-link voltages V_{dc} of the power sources change. Therefore, V_{dc} is used as the trigger for ac power changes.

Second, as low-voltage distribution grids and, thus, microgrid lines are mainly resistive, the active power through a distribution line mainly depends on the voltage amplitude, unlike in transmission grids where the reactive power is mainly linked with the voltage amplitude. Therefore, with this P/V linkage in the microgrid, V_{dc} triggers the rms microgrid voltage V_g to change the ac-power export from the DG unit to the microgrid; this forms the basics of the V_g/V_{dc}-droop control strategy.

Third, microgrids operate with a high share of renewables, which are less controllable than the central generators, and their power should be exploited optimally as long as possible. In current practice, the renewable energy sources are generally not actively dispatched as they operate in maximum power-point tracking (MPPT) unless in emergency situations, such as overvoltage, when they shut down. With the increasing share of renewables, however, dispatching their power will be required for the power system stability, which is specifically valid in small-scale islanded microgrids. Still, changing the output power of the renewables should be delayed compared to the exploitation of the more controllable generators. Therefore, if only the V_g/V_{dc}-droop control is used, the dc power of the DG units is not affected by the power control algorithm of the VSI, only by the generator itself, for example, led by the MPPT algorithm. The implementation of the delayed dc-power changes is discussed in Section III-B.

The V_g/V_{dc}-droop controller of Fig. 3 changes the set value of the rms voltage $V_g^\star$ according to the change in V_{dc} by means of a proportional (P) controller

$$V_g^\star = V_{g,nom} + m(V_{dc} - V_{dc,nom}). \tag{1}$$

Even a slight change of V_g leads to a change of the power delivered to the electrical network. This effect is realized by natural balancing due to resistive loads and microgrid lines.

As in the single-phase microgrid configuration of Fig. 1, the dc-link voltage shows a ripple of twice the fundamental microgrid frequency of 50 Hz, the bandwidth of the P controller is set in order to avoid this ripple occurring in the ac-side microgrid voltage. Therefore, the P controller is operating with a sample rate of 100 Hz. In case of a higher control frequency, other measures would be required to avoid the appearance of the 100-Hz variations of V_{dc} in v_g. Furthermore, a moving average control is included, causing the desired rms microgrid voltage to be a weighting of the output of the controller and the previous value. This moving average control can be seen as a discrete integrating action.

With the V_g/V_{dc}-droop controller, the power sources are not burdened with frequent power changes as the power P_{dc} delivered by the source is not changed by the V_g/V_{dc} droop controller. This is specifically beneficial for renewable power sources as in this way, their energy can be used more optimally. It can also be implemented without the need for transformation to a synchronous dq-reference frame.

B. P/V_g-Droop Control

All electrical equipment in the microgrid is designed to withstand some voltage deviation from its nominal value. Therefore, the microgrid voltage is allowed to vary in a certain tolerated microgrid voltage band, which is used by the V_g/V_{dc}-droop controller for a stable balancing of the microgrid. However, by using the V_g/V_{dc}-droop control strategy solely, voltage-limit violation can occur. Hence, when the voltage exceeds a certain level, which lies between the voltage limits, the power P delivered to the microgrid is changed by other means than by changing V_g. Therefore, the power P_{dc} delivered to the dc link is changed. Changing P_{dc} can be done in several ways. For instance, P_{dc} can be decreased by battery charge-up, by changing the generated power P_{gen}, or by dumping loads. For an increase of P_{dc}, battery charge-down, demand-side management (potentially driven by the emerging smart grid concept) or an increase of P_{gen} can be incorporated in the control. The method of changing the power delivered to the dc link does not inherently change the

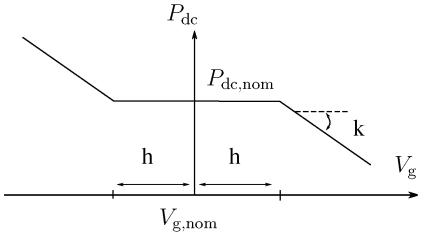

Fig. 4. Combination V_g/V_{dc}-droop and P/V_g-droop.

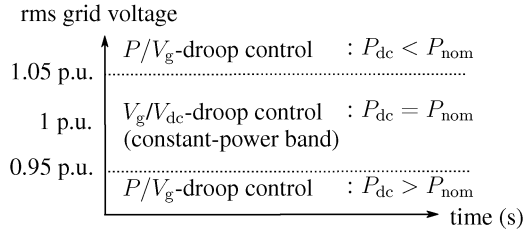

Fig. 5. Control principle for a constant-power band of 5% ($2h = 10\%$): P/V_g-droop and V_g/V_{dc}-droop control.

control method and can be determined according to the specific application.

To control this change of P_{dc}, the V_g/V_{dc}-droop controller cooperates with a P/V_g-droop controller. In the P/V_g-droop control strategy, as depicted in Fig. 3, the power P_{dc} (or dc current I_{dc} in case of a current-controlled source) is changed according to a droop with the microgrid voltage V_g

$$P_{dc} = P_{dc,nom} - k(V_g - V_{g,nom}) \tag{2}$$

with k being a positive droop coefficient and $P_{dc,nom}$ being the nominal value of P_{dc}.

In [17], an analogous approach to delay changing the dc power is made. However, this strategy is based on the P/f linkage, operating on the dc-link voltage and has a storage unit incorporated in the generator, while this paper focusses on the P/V linkage in weak grids, shows a delay depending on the microgrid voltage, and operates with fully distributed generators and storage units. This has advantages concerning the integration of renewable energy sources in the microgrid and for the control of external storage units that can react on the microgrid voltage without the need for communication and can be fully distributed units.

C. Combination V_g/V_{dc} and P/V_g-Droop Control

In a constant-power band, limited by the voltages $V_{g,nom} - h$ and $V_{g,nom} + h$, the V_g/V_{dc}-droop method controls the rms microgrid voltage under constant P_{dc}. If the obtained microgrid voltage V_g surpasses this constant-power band, the P/V_g-droop controller changes P_{dc} as shown in Figs. 4 and 5

$$P_{dc} = P_{nom} - k * a \tag{3}$$

with

$$a = \begin{cases} 0 & \text{if } V_{g,nom} - h \le V_g \le V_{g,nom} + h \\ V_g - (V_{g,nom} + h) & \text{if } V_g > V_{g,nom} + h \\ V_g - (V_{g,nom} - h) & \text{if } V_g < V_{g,nom} - h. \end{cases} \tag{4}$$

By combining the V_g/V_{dc}-droop control with a P/V_g-droop control strategy that changes the generated power (or uses storage), voltage-limit violation is avoided.

The combination of the two control principles V_g/V_{dc}-droop and P/V_g-droop control can be introduced in the microgrid in order to obtain the advantages of both. With the V_g/V_{dc}-droop, the microgrid voltage can be changed by detecting changes of V_{dc}, and balancing is achieved without changing P_{dc}. This is possible as a relatively big difference between the obtained and nominal microgrid voltage is allowed (up to 8% for the 1-min rms voltage and 10% for the 1-s voltage [30]). By using the P/V_g-droop control, P_{dc} can be changed in case the constant-power band is surpassed, increasing the power flexibility in the microgrid and avoiding the voltage-limit violation. An advantage is that by using these two droop controllers, P_{dc} of the generators or storage elements changes less frequently than in the case of P/f or P/V_g-droop control solely.

The width $2h$ of the constant-power band can be set according to the specific characteristics of the power sources. For example, $2h$ can be small for highly controllable sources, which can change their fuel intake rapidly. In this way, the control abilities of these sources are fully exploited. For less-controllable sources, such as many renewables, $2h$ can be larger. With this large constant-power band, the exported power of the renewable energy sources can be changed according to the state of the electrical network while still, this power change is delayed compared to that of other, more controllable power generators. Otherwise, a less optimal exploitation of the available renewable energy would be obtained.

D. Conclusion

By combining the V_g/V_{dc} and P/V_g-droop controllers, the advantages of both control strategies can be exploited, frequent power changes are avoided, no communication for the primary control is required, and the tolerated voltage deviation from its nominal value is effectively used for the control. Also, both controllers take the specific characteristics of the islanded microgrid into account, such as the lack of inertia, resistive lines, and high share of renewables.

IV. One Power Source

The V_g/V_{dc}-droop control principle is applied to a microgrid, that, in this first simulation, is fed by one power source. Also, the P/V_g-droop control strategy is included and the application of a constant-power band and its advantages are shown in a simulation example.

A. V_g/V_{dc}-Droop Controller

In the first simulation, the islanded microgrid consists of a line resistance $R_l = 0.3\,\Omega$ in series with a load $R = 33\,\Omega$. The controller filter parameters are $L = 2$ mH and $C = 3\,\mu$F and only the V_g/V_{dc}-droop control is used in this simulation. The nominal dc-link voltage $V_{dc,nom}$ is equal to 450 V and $C_{dc} = 1.5$ mF. Note that the simulations are performed up to the level of the switches, including switching ripple, but the plots are sampled

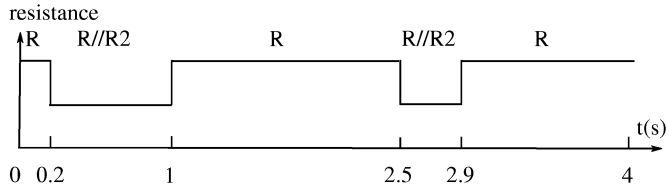

Fig. 6. Timeline of the change of load resistance.'//' denotes "in parallel."

with the switching frequency since this is also the case for the VSI control and measurements. The reference microgrid voltage $v_{\mathrm{g}}^{\star}$ is a 50-Hz voltage, with an initial rms value of 230 V. The power P_{dc} delivered by the source is constant and is equal to 2100 W in this first simulation. In order to study the controller performance to large transients, a variable load is implemented (e.g., after 0.2 s, a second load R_2 of 33 Ω is turned on in parallel with R). The time line of Fig. 6 shows the load change in the microgrid. For verification of the $V_{\mathrm{g}}/V_{\mathrm{dc}}$-droop control strategy, the theoretical steady-state microgrid voltage can be calculated (e.g., for a microgrid loaded with R)

$$P = \frac{V_{\mathrm{g}}^2}{R_{\mathrm{tot}}} = \frac{V_{\mathrm{g}}^2}{(R + R_l)}. \tag{5}$$

Thus, $V_{\mathrm{g}} = 264.4$ V. If R_2 is turned on in parallel with R: $V_{\mathrm{g}} = 187.8$ V. This voltage is lower than in the first case with only R because the power delivered by the source remains the same with a lower overall microgrid impedance.

The simulation results of the rms microgrid voltage V_{g} are depicted in Fig. 7(a). The changes of the rms voltage due to the variations of the load resistance are clearly shown in this figure. The power P delivered to the microgrid is shown in Fig. 7(b). Accurate information about active power is only possible after one fundamental period of 0.02 s; hence, the initial value of zero. From this figure, it is concluded that during steady state, P is constant and equal to the output power P_{dc} of the power source. During load changes, transients in the power P delivered to the microgrid occur because the $V_{\mathrm{g}}/V_{\mathrm{dc}}$-droop controller has a finite bandwidth. For example, at a time $t = 1$ s, when R_2 turns off, the overall microgrid resistance increases. The microgrid voltage remains constant just after the transient because the P controller operates at 100-Hz frequency. To maintain the power balance between the power source and the rest of the microgrid, some power is being delivered to the dc-link capacitor C_{dc}. Therefore, the dc-link voltage increases and the $V_{\mathrm{g}}/V_{\mathrm{dc}}$-droop controller reacts. It increases the set value of V_{g} until no more power is exchanged with C_{dc}, and V_{dc} remains constant. Subsequently, again a steady state is reached and the power P delivered to the electrical network is equal to the dc power P_{dc}. The theoretically calculated rms voltages match the simulation results of Fig. 7(a). These voltages are larger than those generally tolerated in microgrids since power flexibility is not yet included in this simulation example.

B. $V_{\mathrm{g}}/V_{\mathrm{dc}}$ and P/V_{g}-Droop Controller

In the previous simulation, it is shown that with the $V_{\mathrm{g}}/V_{\mathrm{dc}}$-droop controller, stable microgrid operation is obtained. However, in order to avoid voltage-limit violation, also

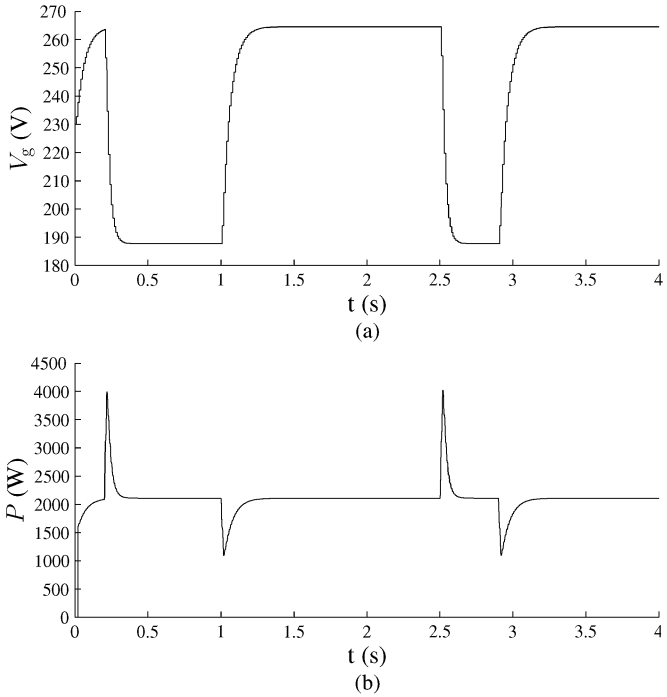

Fig. 7. One power source: $V_{\mathrm{g}}/V_{\mathrm{dc}}$-droop control. (a) RMS microgrid voltage v_{g}. (b) Power delivered to the microgrid.

a P/V_{g}-droop controller is included in this simulation. The simulations with the combined $V_{\mathrm{g}}/V_{\mathrm{dc}}$-droop and P/V_{g}-droop control strategies are again performed with $P_{\mathrm{dc}} = 2100$ W, $R_l = 0.3\ \Omega$, $R = 33\ \Omega$, and $R_2 = 33\ \Omega$, which turns on in parallel with R according to Fig. 6. The results for different widths $2h$ of the constant-power band are studied. In the simulation of Fig. 7, P_{dc} was constant as the P/V_{g}-droop was turned off or the constant-power band was very wide (e.g., $h = 20\%$), resulting in no change of P_{dc}. As in the latter control, the voltage limits can be exceeded, the P/V_{g}-droop is turned on in the next simulation. For the case of h being equal to 5%, the simulated microgrid rms voltage and delivered power are shown in Fig. 8(a) and (b), respectively. In Fig. 8(a) (e.g., at $t = 1.5$ s), the power P is less than the nominal power of 2100 W. Also, the rms microgrid voltage is less than the voltage obtained in Fig. 7(a), where P remained constant and where overvoltage conditions occurred. Therefore, it is shown that in the case of overvoltage, lowering P_{dc} by means of the P/V_{g}-droop control, indeed benefits the microgrid control. When using a smaller constant-power band, the microgrid voltage will be closer to its nominal value as is shown in Fig. 8(a) and (c). However then, the dc power will be forced further away from its nominal value, which is often the optimal value. Therefore, for example, renewables have a large constant-power band $2h$, while more controllable units have a lower constant-power band.

In conclusion, power control of the generators in islanded microgrids can be achieved by using a combination of the two control strategies, which are: 1) $V_{\mathrm{g}}/V_{\mathrm{dc}}$-droop and 2) P/V_{g}-droop control. In the constant-power band, P_{dc} remains constant and the power flow to the microgrid is controlled by means of the $V_{\mathrm{g}}/V_{\mathrm{dc}}$-droop controller only. The power P_{dc} is only changed in case V_{g} surpasses this constant-power band and then, the

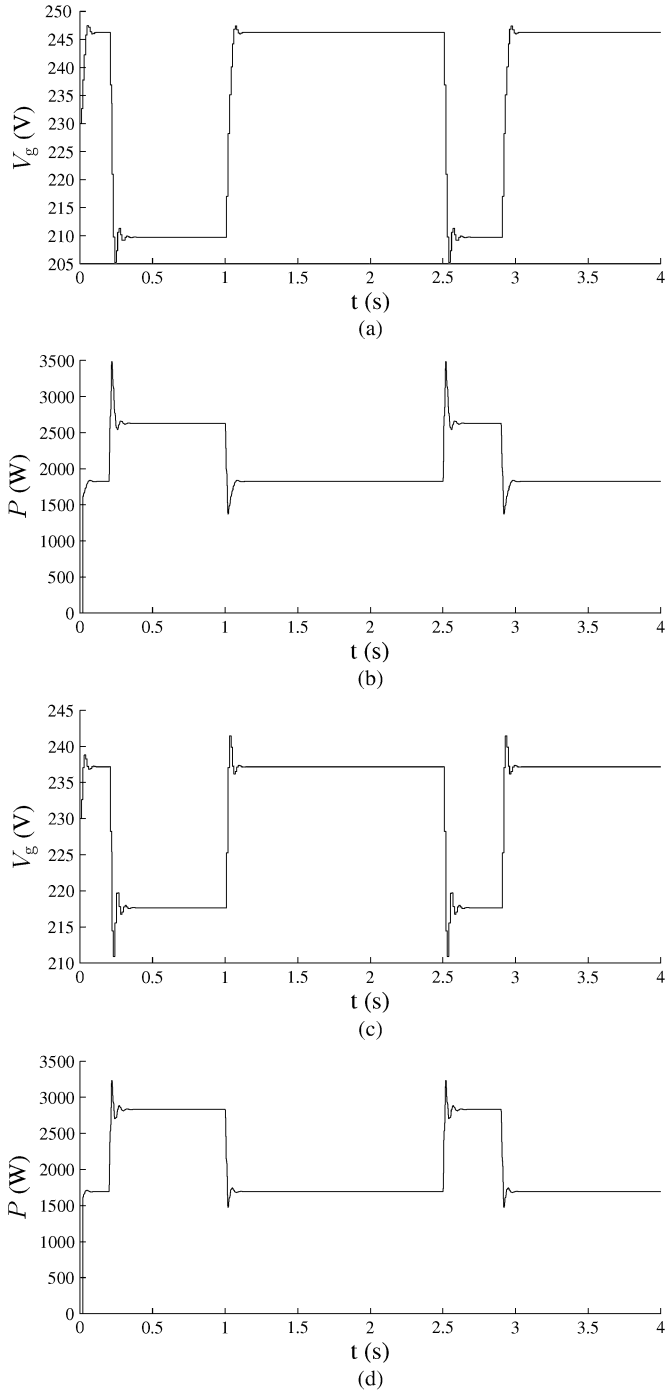

Fig. 8. One power source V_g/V_{dc}-droop control, with P/V_g-droop turned on and with different constant-power bands $2h$. (a) RMS microgrid voltage V_g (1: large constant-power band). (b) power P delivered to the microgrid (1). (c) RMS microgrid voltage V_g (2: small constant-power band). (d) Power P delivered to the microgrid (2).

P/V_g-droop control is turned on. Furthermore, the width of the constant-power band can be set according to the characteristics of the power source in order to avoid frequent power changes or to fully exploit the control abilities of the power sources.

V. Multiple Power Sources

By using Fig. 9, the principle of power sharing for the case of two (or more) power sources will be addressed. For example,

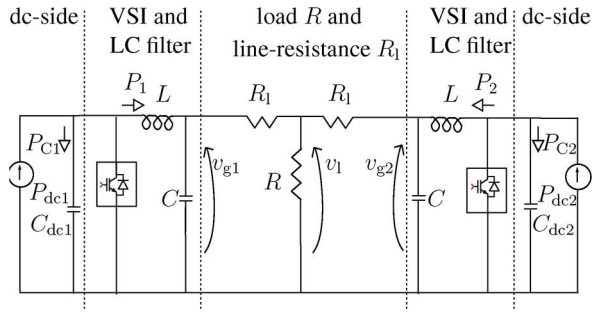

Fig. 9. Two VSIs: power-sharing principle and configuration of the microgrid.

first, only one power source with power P_{dc1} is turned on. The V_g/V_{dc}-droop controller of this power source controls the rms voltage to V_{g1} in order to achieve a constant dc-link voltage, and $V_{g1} > V_l$, with V_l the rms value of the load voltage v_l. As the second DG unit is turned off, in open circuit, V_{g2} is equal to V_l. Next, the second source with power P_{dc2} turns on. At first, V_{g2} remains constant and is equal to V_l and, therefore, P_2 remains zero. In order to maintain the power balance, the dc-link voltage V_{dc2} increases because the dc-link capacitor power P_{C2} is equal to P_{dc2}. Therefore, the V_g/V_{dc}-droop control of this second source changes the set value of V_{g2}. Power is injected to the rest of the microgrid and V_{g2} increases. The power delivered to the load, here represented as R, increases and, therefore, the voltage V_l will increase. If V_{g1} remains constant, the power P_1 delivered to the microgrid by source 1 decreases as the difference $(V_{g1} - V_l)$ is lower. Therefore, under constant P_{dc1}, the dc-link voltage of source 1 will increase and the controller will increase V_{g1}. This process goes on until steady state is reached. The steady-state value of V_l will be larger than in the case with only source 1.

If a certain voltage level is surpassed, this control can also be extended with P/V_g-droop control to change P_{dc} analogously as in the case of a single power source.

A. V_g/V_{dc}-Droop Controller

The microgrid configuration depicted in Fig. 9 is simulated. Two constant-power sources P_{dc1} and P_{dc2}, generating 700 W and 1400 W, respectively, are active. Both have a dc-link capacitor with voltage V_{dc1} and V_{dc2} and control the microgrid voltages v_{g1} and v_{g2} by means of a VSI. Theoretically, for the given parameters and with a load R of 33 Ω, in steady-state conditions, $V_{g,1} = 264$ V and $V_{g,2} = 268$ V are calculated. V_{g2} is larger than V_{g1} as $P_2 > P_1$.

First, the microgrid is simulated with a constant impedance load. The rms microgrid voltages V_{g1} and V_{g2} are depicted in Fig. 10(a). The power sources obtain microgrid voltages that are equal to the theoretically calculated values. The power delivered to the microgrid is equal to the nominal power of 700 W and 1400 W, except during startup as is shown in Fig. 10(b). Again, only after one fundamental period of 20 ms, valid active power determination can be expected; hence, the initial value of zero. The dc-link voltage of source 1 is depicted in Fig. 10(c). Note the small scope in the V_{dc}-axis of this figure. A small 100-Hz V_{dc} ripple of less than 1% is

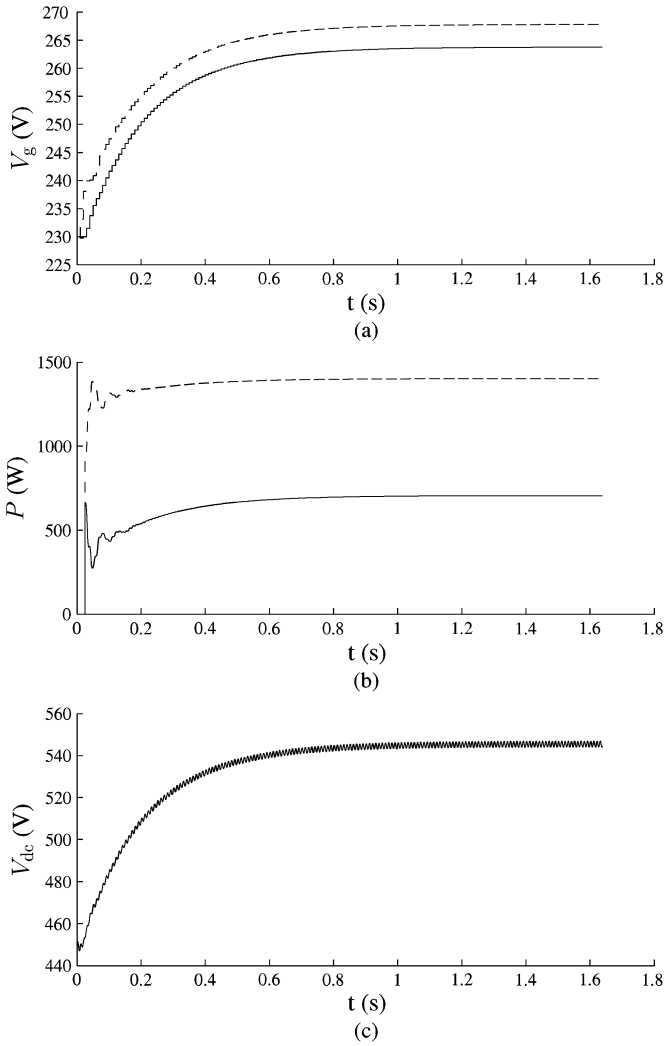

Fig. 10. Two power sources: 1) V_g/V_{dc}-droop control, constant load and 2) P/V_g-droop control turned off (— = VSI 1, --- = VSI 2). (a) RMS microgrid voltage V_g. (b) Power P delivered to the microgrid. (c) DC-link voltage of source 1.

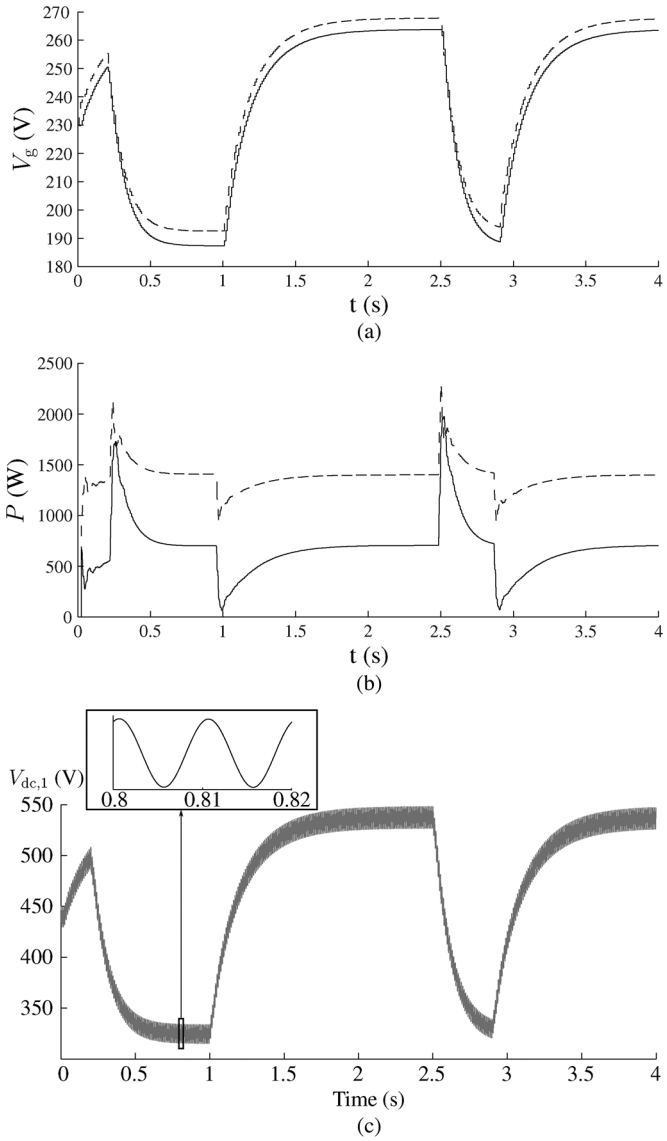

Fig. 11. Two power sources: 1) V_g/V_{dc}-droop control, variable load and 2) P/V_g-droop control turned off (— = VSI 1, --- = VSI 2). (a) RMS microgrid voltage V_g. (b) Power P delivered to the microgrid. (c) DC-link voltage of source 1.

obtained. Stable operation is shown, but V_g becomes large as the P/V_g control is not yet active.

Second, the microgrid is simulated with a variable load. The load changes follow the pattern depicted in Fig. 6, with $R = 33\ \Omega$ and $R_2 = 33\ \Omega$. The microgrid rms voltages V_{g1} and V_{g2} are depicted in Fig. 11(a). The power P delivered to the microgrid is equal to the nominal power of 700 W and 1400 W, except during the load changes. It is shown in Fig. 11(b) that if the second load is turned on, the power delivered to the microgrid increases instantly due to the lower load resistance and the relatively slow V_g/V_{dc}-droop control. This power originates from the dc-link capacitor, lowering its voltage. The V_g/V_{dc}-droop control of the two sources then reduces the microgrid voltage to obtain a constant dc-link voltage. The dc-link voltage of the first source is depicted in Fig. 11(c). It is shown that the reference voltage of 450 V is not exactly matched. This is due to the use of a P controller. Note that by changing the droop of this controller, V_{dc} can be forced closer to its nominal value, depending on the specifications of the dc link. Furthermore, the 100-Hz variation of the dc-link voltage is clearly shown.

In these simulation cases, the obtained voltages exceed the voltage limits since no power flexibility is incorporated in the control. Therefore, the P/V_g-droop controller is included in the next simulation.

B. V_g/V_{dc} and P/V_g-Droop Controller

In order to limit the microgrid voltage, the P/V_g-droop principle is applied to change P_{dc}, also in case of multiple inverters. In this simulation, again, the load consists of $R = 33\ \Omega$ and another load $R_2 = 33\ \Omega$ turns on and off according to Fig. 6.

In Fig. 11(a), the obtained rms microgrid voltage is depicted for the case of no P/V_g-droop and in Fig. 12(a) for the case with P/V_g-droop and a constant-power band of 5%. The droop controller forces the voltage closer to the nominal value of 230

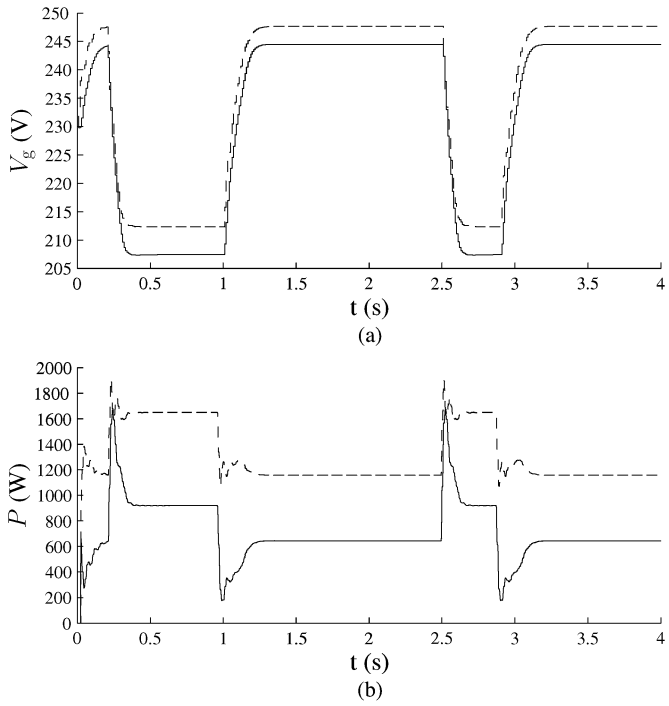

Fig. 12. Two sources: 1) variable load, with V_g/V_{dc} and 2) P/V_g-droop control (— = VSI 1, --- = VSI 2). (a) RMS microgrid voltage V_g. (b) Power P delivered to the microgrid.

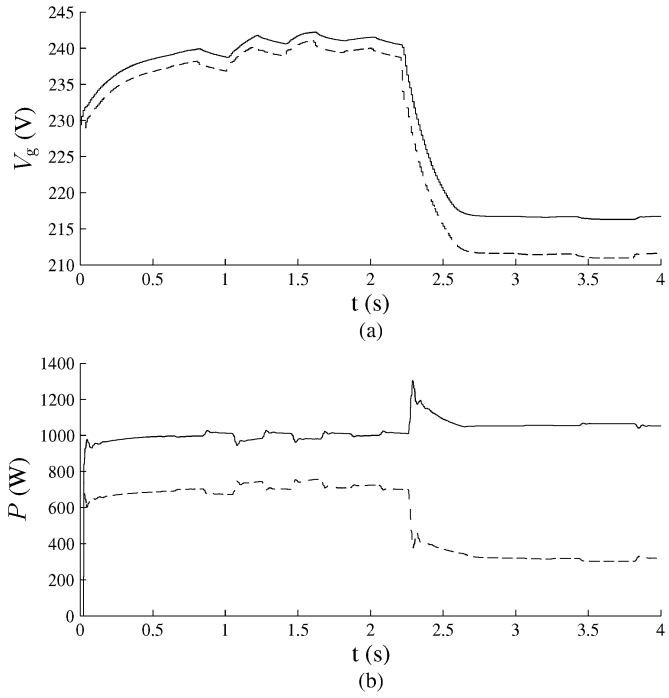

Fig. 13. Two sources (including the variable output of PV panel), constant load, with V_g/V_{dc} and P/V_g-droop control (— = VSI 1, --- = VSI 2). (a) RMS microgrid voltage V_g. (b) Power P delivered to the microgrid.

V. The delivered powers without and with the P/V_g-droop controller are depicted in Figs. 11(b) and 12(b), respectively. It is shown in Fig. 12(b) that by implementing the P/V_g-droop (e.g., under high voltages), the delivered power is lower than the nominal power to force the voltage closer to its nominal value, depending on the droop.

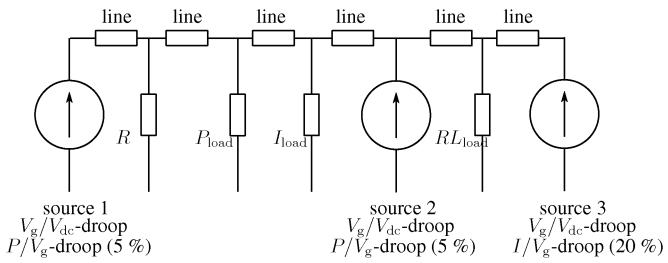

Fig. 14. Three VSIs and different loads: constant-power and current loads.

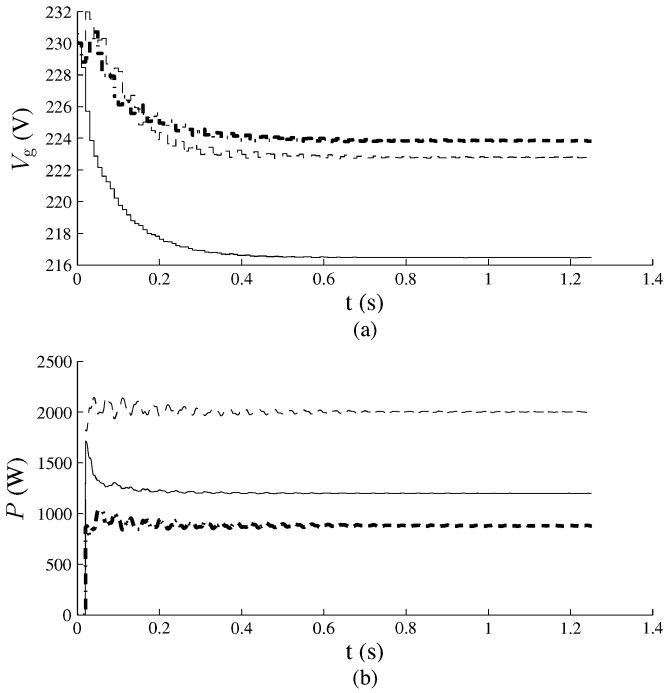

Fig. 15. Extended microgrid: three power sources, R and RL loads, constant-power load, and constant-current load (— = VSI 1, --- = VSI 2, -.-.- = VSI 3). (a) RMS microgrid voltage V_g. (b) Active power P delivered to the microgrid.

The same is also simulated where VSI 2 is a current-controlled source, with varying current:

- $t = 0$ s to $t = 0.5$ s: $I = I_{nom}$;
- $t = 0.5$ s to $t = 2$ s: $I = I_{nom} + I_{var}$;
- $t = 2$ s to $t = 2.2$ s: $I = I_{nom}$;
- $t = 2.2$ s to $t = 3$ s: $I = I_{nom}/2$;
- $t = 3$ s to $t = 3.8$ s: $I = I_{nom}/2 + I_{var}$

where I_{var} is a randomly varying component (e.g., PV panel with time-varying irradiation) with maximum 10% of I_{nom} and I_{nom} being equal to 1.5 A. Only VSI 1 is equipped with the P/V_g-droop control and $P_{dc,nom1} = 1000$ W. For VSI 2, this droop control is only activated with a large constant-power band since this represents a renewable energy source. To clearly show the effect of this varying output power, the load remains constant and is equal to R. The simulation results are depicted in Fig. 13. From $t = 0$ s to $t = 0.5$ s, the startup transient is shown. Then, because of the ripple in the generated power of VSI 2, a ripple

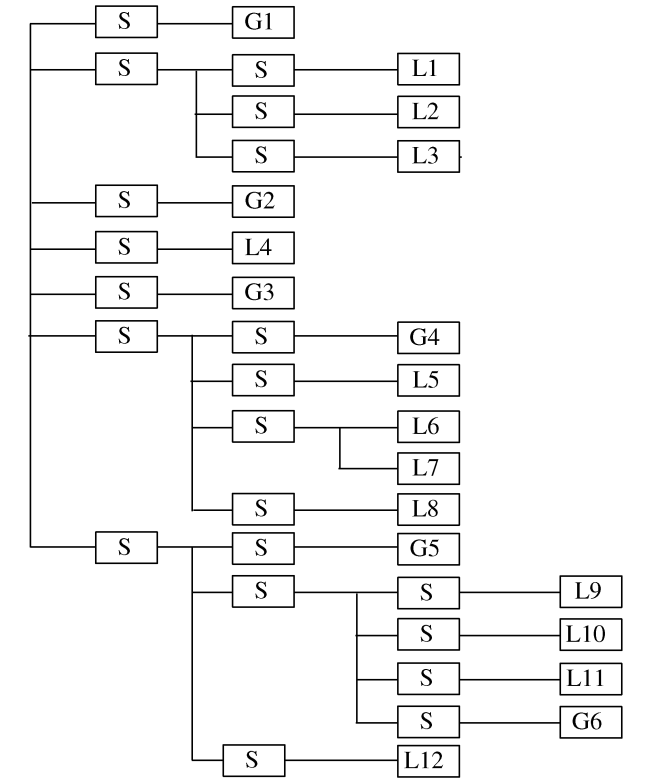

Fig. 16. Configuration of a realistic case of a microgrid.

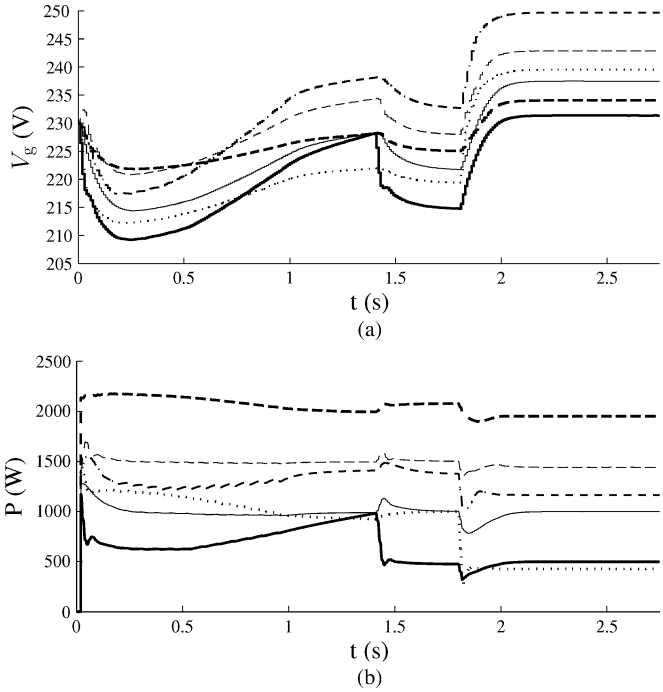

Fig. 17. Real microgrid: six power sources, R and RL loads, constant-power load and constant-current load, variable sources and loads (— = VSI 1, - - - = VSI 2, — = VSI 3, - - - = VSI 4, -.-.- = VSI 5, . . . = VSI 6). (a) RMS microgrid voltage V_g. (b) Active power P delivered to the microgrid.

in the output power P and the microgrid voltage is depicted. Still, stable operation is obtained, and the changes of power of VSI 2 are mainly delivered by VSI 1. At $t = 2.2$ s, the output power of VSI 2 significantly decreases, which is also depicted in the microgrid voltage. It is also shown that the VSI 1 then increases its output power since the constant-power band of 5% is exceeded.

Also, the simulation case is extended to an islanded microgrid consisting of three power sources depicted in Fig. 14. One of these sources is a current-controlled source with the V_g/V_{dc}-droop control strategy and the I/V_g-droop control, which is analogous to P/V_g-droop control, with a wide constant-power band $2h = 20\%$. The other two power sources use a combination of the V_g/V_{dc} and P/V_g-droop control principles with a constant-power band $2h$ of 10%. The nominal power of sources 1 and 2 is equal 1.2 and 2 kW, respectively, while source 3 has current $I_{dc,nom} = 2$ A for a nominal dc-link voltage of 450 V. In this simulation, the loads consist of a combination of R, RL loads, a constant-power load (P_{load}), and a constant-current load (I_{load}). Due to the inductive load, reactive power control in a Q/f-droop according to [22], [23] is also included in this simulation. This droop controller takes the mainly resistive nature of the microgrid lines into account and operates without interunit communication, like the active power controllers. The simulation results are depicted in Fig. 15. It is shown that stable operation is obtained in the extended microgrid. The terminal rms voltage of power source three is larger than that of the other two as, in this simulation, the main part of the load is located between the first two sources.

Finally, a more realistic microgrid case is simulated, and the microgrid configuration is depicted in Fig. 16. The microgrid consists of different types of DG units. They vary to the extent in which they are controllable; thus, the constant-power band $2h$ varies. Also, current-controlled and power-controlled sources are included. Furthermore, a dynamical current-controlled source G3, such as a PV panel, thus changing its dc current, is included in the simulation. This current source delivers 1.5-A dc current from $t = 0$ s until $t = 0.5$ s and then it has a linearly increasing dc current until, at $t = 1.4$ s, the dc current $I_{dc,3}$ is equal to 2.22 A. At $t = 1.4$ s, its output drops to 1.11 A. The details of the other generators are shown in Fig. 16, with

nominal values $P_{\mathrm{nom},1} = 1000$ W, $P_{\mathrm{nom},2} = 1500$ W, $P_{\mathrm{nom},4} = 2000$ W, $I_{\mathrm{nom},5} = 3$ A, and $P_{\mathrm{nom},6} = 700$ W. Also, a combination of different loads is included, such as constant power loads, current loads, RL loads, and nonlinear loads (NLL) represented as single-phase rectifiers. The NLL L_4 and the RL load L_9 turn off after $t = 1.8$ s. From $t = 0$ s to $t = 1$ s, the variable resistive load L_{12} increases in discrete steps, from 500 to 36 Ω. The simulation results are depicted in Fig. 17.

From this simulation, its is concluded that stable operation is obtained. From 0 to 1.4 s, the linear increase of the output power of generator 3 is clearly shown in P and V_{g}. As the load L_{12} linearly increases as well from $t = 0$ s to $t = 1$ s, the other power sources do not change their output power much in this time interval. When generator 3 drops at $t = 1.4$ s, a small transient in power where all other generators slightly increase their output power and a small voltage decrease are clearly shown. At $t = 1.8$ s, when two loads turn off, a clear increase in V_{g} and a transient are shown in the simulation. At the end of the simulation, clearly the output power of the generators is strongly linked with their generated power $P_1 \approx 1000$ W, $P_2 \approx 1500$ W, $P_3 \approx 600$ W, $P_4 \approx 2000$ W, $P_5 \approx 1350$ W, $P_6 \approx 600$ W, and the slight changes are obtained by the P/V_{g}-droop controllers.

From these simulations, it is concluded that the controllers obtain a stable islanded microgrid operation, share power according to the ratings of the sources, limit the voltage, take the specific characteristics of the sources into account by setting the constant-power band, and do no require interunit communication.

VI. Conclusion

In this paper, the $V_{\mathrm{dc}}/V_{\mathrm{g}}$-droop control principle is presented for the control of generators in an islanded microgrid. This control strategy focusses on the specific properties of the microgrid since it takes the P/V_{g}-linkage in the microgrid into account, its lack of inertia, and the dc-link capacitor storage of the power-electronic interface. Furthermore, to avoid voltage-limit violation, a P/V_{g}-droop control strategy is implemented. The microgrid control with one power source is studied, next to the microgrid control and power sharing with multiple power sources, and good results are obtained. Furthermore, the simulation results with only the $V_{\mathrm{g}}/V_{\mathrm{dc}}$-droop control are compared with results where the P/V_{g}-droop is turned on.

It is shown that proper power sharing and balancing in islanded microgrids can be achieved without communication by using a combination of $V_{\mathrm{g}}/V_{\mathrm{dc}}$ and P/V_{g}-droop control. The $V_{\mathrm{g}}/V_{\mathrm{dc}}$-droop avoids the frequent changes of the delivered power, which are obtained with the conventional P/f or P/V_{g}-droop control. For this reason, the P/V_{g}-droop controller is only turned on in case the voltage exceeds the constant-power band. Furthermore, for optimally exploiting the power sources in the microgrid, the width of this band can be set according to the characteristics of the DG unit. With the highly increased penetration of renewable energy sources in the grid, exploiting them all and always in the MPPT condition is no longer sustainable, and storage is also limited, certainly in small islanded microgrids. Therefore, their exported power will need to change according to the state of the electrical network. However, it is beneficial to delay this power change compared to other, more controllable power generators. In this paper, it is shown that the constant-power band offers a solution for this if a large band is included in renewables. More controllable units, on the other hand, have a smaller constant-power band to exploit their power flexibility.

References

[1] C. Marnay and G. Venkataramanan, "Microgrids in the evolving electricity generation and delivery infrastructure," presented at the IEEE Power Eng. Soc. Gen. Meeting, Montréal, QC, Canada, Jun. 18–22, 2006.

[2] R. H. Lasseter, A. Akhil, C. Marnay, J. Stephens, J. Dagle, R. Guttromson, A. Meliopoulous, R. Yinger, and J. Eto, "The CERTS microgrid concept, white paper on integration of distributed energy resources," LBNL-50829, California Energy Comm., Office of Power Technologies—U.S. Dept. Energy, Apr. 2002. [Online]. Available: http://certs.lbl.gov

[3] R. H. Lasseter and P. Paigi, "Microgrid: A conceptual solution," presented at the IEEE Power Electron. Spec. Conf. Aachen, Germany, 2004.

[4] N. Pogaku, M. Prodanović, and T. C. Green, "Modeling, analysis and testing of autonomous operation of an inverter-based microgrid," *IEEE Trans. Power Electron.*, vol. 22, no. 2, pp. 613–625, Mar. 2007.

[5] M. A. Pedrasa and T. Spooner, "A survey of techniques used to control microgrid generation and storage during island operation," presented at the Australian Universities Power Engineering Conf., Dec. 10–13, 2006.

[6] F. Katiraei, M. R. Iravani, and P. W. Lehn, "Micro-grid autonomous operation during and subsequent to islanding process," *IEEE Trans. Power Del.*, vol. 20, no. 1, pp. 248–257, Jan. 2005.

[7] T. C. Green and M. Prodanovíc, "Control of inverter-based microgrids," *Elect. Power Syst. Res.*, vol. 77, no. 9, pp. 1204–1213, Jul. 2007.

[8] F. Katiraei, R. Iravani, N. Hatziargyriou, and A. Dimeas, "Microgrids management: Controls and operation aspects of microgrids," *IEEE Power Energy Mag.*, vol. 6, no. 3, pp. 54–65, May/Jun. 2008.

[9] S. Barsali, M. Ceraolo, P. Pelacchi, and D. Poli, "Control techniques of dispersed generators to improve the continuity of electricity supply," in *Proc. IEEE Power Eng. Soc. Winter Meeting*, 2002, pp. 789–794.

[10] J. A. Peças Lopes, C. L. Moreira, and F. O. Resende, "Microgrids black start and islanded operation," presented at the 15th Power Systems Computation Conf., Liège, Belgium, Aug. 22–26, 2005.

[11] A. L. Dimeas and N. D. Hatziargyriou, "Operation of a multiagent system for microgrid control," *IEEE Trans. Power Syst.*, vol. 20, no. 3, pp. 1447–1455, Aug. 2005.

[12] P. M. Costa and M. A. Matos, "Assessing the contribution of microgrids to the reliability of distribution networks," *Elect. Power Syst. Res.*, vol. 79, no. 2, pp. 382–389, Feb. 2009.

[13] A. Engler, O. Osika, M. Barnes, and N. Hatziargyriou, DB2 evaluation of the local controller strategies. Jan. 2005. [Online]. Available: www.microgrids.eu/micro2000

[14] M. Marwali, J.-W. Jung, and A. Keyhani, "Control of distributed generation systems—Part II: Load sharing control," *IEEE Trans. Power Electron.*, vol. 19, no. 6, pp. 1551–1561, Nov. 2004.

[15] M. C. Chandorkar, D. M. Divan, and R. Adapa, "Control of parallel connected inverters in standalone ac supply systems," *IEEE Trans. Ind. Appl.*, vol. 29, no. 1, pp. 136–143, Jan./Feb. 1993.

[16] K. Debrabandere, B. Bolsens, J. Van den Keybus, A. Woyte, J. Driesen, and R. Belmans, "A voltage and frequency droop control method for parallel inverters," *IEEE Trans. Power Electron.*, vol. 22, no. 4, pp. 1107–1115, Jul. 2007.

[17] F. A. Bhuiyan and A. Yazdani, "Multimode control of a DFIG-based wind-power unit for remote applications," *IEEE Trans. Power Del.*, vol. 24, no. 4, pp. 2079–2089, Oct. 2009.

[18] C. Sao and P. Lehn, "Intentional islanded operation of converter fed microgrids," presented at the IEEE Power Eng. Soc. Gen. Meeting, Montreal, QC, Canada, Jun. 18–22, 2006.

[19] C. Sao and P. Lehn, "Control and power management of converter fed microgrids," *IEEE Trans. Power Syst.*, vol. 23, no. 3, pp. 1088–1098, Aug. 2008.

[20] T. L. Vandoorn, B. Renders, L. Degroote, B. Meersman, and L. Vandevelde, "Grid voltage control in islanded microgrids with inverter-interfaced power sources," presented at the 2nd Innovation for Sustainable Production Conf., Bruges, Belgium, Apr. 18–21, 2010.

[21] T. L. Vandoorn, B. Renders, F. M. L. L. De Belie, B. Meersman, and L. Vandevelde, "A voltage-source inverter for microgrid applications with an inner current control loop and an outer voltage control loop," presented at the Int. Conf. Renewable Energies and Power Quality, Valencia, Spain, Apr. 14–17, 2009.
[22] H. Laaksonen, P. Saari, and R. Komulainen, "Voltage and frequency control of inverter based weak LV network microgrid," presented at the Int. Conf. Future Power Systems, Amsterdam, The Neherlands, Nov. 18, 2005.
[23] T. L. Vandoorn, B. Renders, B. Meersman, L. Degroote, and L. Vandevelde, "Reactive power sharing in an islanded microgrid," presented at the 45th Int. Universities Power Engineering Conf., Cardiff, Wales, U.K., Aug. 31–Sep. 3 2010.
[24] F.-S. Pai and S.-J. Huang, "A detection algorithm for islanding-prevention of dispersed consumer-owned storage and generating units," *IEEE Trans. Energy Convers.*, vol. 16, no. 4, pp. 346–351, Dec. 2001.
[25] M. A. Redfern and G. Fielding, "Protection against loss of utility grid for a dispersed storage and generation unit," *IEEE Trans. Power Del.*, vol. 8, no. 3, pp. 948–954, Jul. 1993.
[26] Y. Li, D. M. Vilathgamuwa, and P. C. Loh, "Design, analysis, and real-time testing of a controller for multibus microgrid system," *IEEE Trans. Power Electron.*, vol. 19, no. 5, pp. 1195–1204, Sep. 2004.
[27] F. Gao and M. R. Iravani, "A control strategy for a distributed generation unit in grid-connected and autonomous modes of operation," *IEEE Trans. Power Del.*, vol. 23, no. 2, pp. 850–859, Apr. 2008.
[28] P. Arboleya, D. Diaz, J. M. Guerrero, P. Garcia, F. Briz, C. Gonzalez-Moran, and J. G. Aleisxandre, "An improved control scheme based in droop characteristic for microgrid converters," *Elect. Power Syst. Res.*, vol. 80, no. 10, pp. 1215–1221.
[29] J. C. Vasquez, J. M. Guerrero, A. Luna, P. Rodriguez, and R. Teodorescu, "Adaptive droop control applied to voltage-source inverters operating in grid-connected and islanded modes," *IEEE Trans. Ind. Electron.*, vol. 56, no. 10, pp. 4088–4096, Oct. 2009.
[30] M. Bollen, J. Zhong, O. Samuelsson, and J. Björnstedt, "Performance indicators for microgrids during grid-connected and island operation," presented at the IEEE Power Tech. Conf., Bucharest, Romania, Jun, 28–Jul. 2 , 2009.

Tine L. Vandoorn (S'09) was born in Torhout, Belgium, in 1985. She received the M.S. degree in electromechanical engineering from Ghent University, Ghent, Belgium, in 2008, where she is currently pursuing the Ph.D. degree.

Her research interests include voltage and power control of microgrids and smart microgrids.

Ms. Vandoorn received a grant as Ph.D. Fellow of the Research Foundation-Flanders.

Bart Meersman (S'07) was born in Sint-Niklaas, Belgium, on July 29, 1983. He received the M.S. degree in electromechanical engineering from Ghent University, Ghent, Belgium, in 2006, where he is currently pursuing the Ph.D. degree.

Currently, he is with the Department of Electrical Energy, Electrical Energy Laboratory, Systems and Automation (EESA), Ghent University. His research interests include dynamic phasors, renewable energy applications, digital control of power-electronic converters, and their contribution to power quality.

Lieven Degroote (S'07) was born in Roeselare, Belgium, on July 6, 1982. He received the M.S. and Ph.D. degrees in electromechanical engineering from Ghent University, Ghent, Belgium, in 2005 and 2010, respectively.

Currently, he is with the Department of Electrical Energy, Electrical Energy Laboratory, Systems and Automation (EESA), Ghent University. His research interests include transformers, harmonic analysis of distribution networks, network losses, and the influence of power-electronic inverters on power quality.

Bert Renders (S'06–M'09) was born in Ghent, Belgium, in 1981. He received the M.S. and Ph.D. degrees in electromechanical engineering from Ghent University, Ghent, Belgium, in 2004 and 2009, respectively.

Since then, he has been with the Department of Electrical Energy, Electrical Energy Laboratory, Systems and Automation (EESA), Ghent University. His research interests include digital control of converter-connected distributed generation units and their contribution to power quality.

Lieven Vandevelde (M'05–SM'07) was born in Eeklo, Belgium, in 1968. He received the Ph.D. degree from Ghent University, Ghent, Belgium, in 1997.

Currently, he is with the Department of Electrical Energy, Electrical Energy Laboratory, Systems and Automation (EESA), Ghent University. Since 2004, he has been a Professor of electrical power engineering. His research and teaching activities are in the field of electric power systems, electrical machines, and (computational) electromagnetics.